MECHANISMS OF UNIDIRECTIONAL BLOCK IN CARDIAC TISSUES

RONALD W. JOYNER, *Department of Physiology and Biophysics, University of Iowa, Iowa City, Iowa 52242 U.S.A.*

ABSTRACT We used numerical solutions for cable equations representing nonuniform cardiac strands to investigate possible mechanisms of unidirectional block (UB) of action potential propagation. Because the presence of UB implies spatial asymmetry in some property along the strand, we varied membrane properties ($\bar{g}_{Na}$ or leakage conductance), cell diameter, or intercellular resistance as functions of distance such that a propagating action potential encountered the parameter changes either gradually or abruptly. For changes in membrane properties there was very little difference in the effects on propagation for the gradual or abrupt encounter; but, for changes in cell diameter or in intercellular resistance, there were large differences leading to the production of UB over a wide range of parameter values.

INTRODUCTION

The phenomenon of unidirectional block (UB) of propagating cardiac action potentials has been observed in many experimental preparations since its description by Schmitt and Erlanger in 1928. Various explanations for the mechanisms of arrhythmias have included UB resulting either from the asymmetrical anatomical structure of special regions or from asymmetrical depression of excitability of myocardial tissue. One of the common ways of explaining reentry is to have a ring of tissue with a single area of UB which prevents collision and extinction of an action potential entering the ring and thus establishes a "circus movement" of excitation (Cranefield et al., 1973). UB has also been invoked to explain the protection of parasystolic focus from extrinsic impulses (Watanabe, 1971) and various arrhythmias involving the AV node (Scherf and Cohen, 1964).

Experimental preparations exhibiting UB include the Purkinje-myocardial junction (Mendez et al., 1969), isolated atrial tissue with two pieces connected by a narrow isthmus (De la Fuente et al., 1971), cardiac strands with asymmetrical lesions (Mendez et al., 1969; Downar and Waxman, 1976), cardiac strands positioned asymmetrically across a sucrose gap (Jalife and Moe, 1976; 1979), and an electrical cable representation for a cardiac strand (van Capelle and Janse, 1976). The proposed mechanisms for UB are diagrammed in Fig. 1. In UB type I, the tissue has an inherent difference in safety factor for propagation left to right vs. right to left because of a transition in geometrical properties. We have drawn this change as an increase in effective radius for the cable representation, but the essential feature is a change in electrical load seen by a propagating action potential, and this could result from an actual change in the radius of the cells of the syncytium or by a change in the amount of intercellular coupling (cf., the "funnel hypothesis" of Mendez et al., 1979, for UB at the Purkinje-myocardial junction).

Propagation failure has been produced in squid axons by this mechanism either by inserting

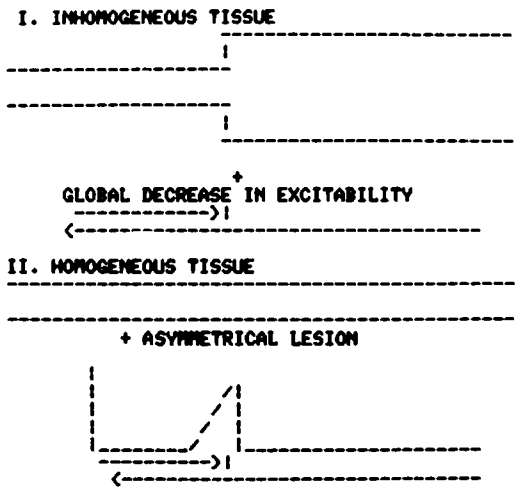

FIGURE 1 Diagram of two general mechanisms for production of unidirectional block (see text).

a low resistance wire into a part of the axon (Ramon et al., 1976) or when an action potential initiated in a small branch propagated back to the large main axon (Westerfield et al., 1978; Joyner et al., 1978). Abnormal production of UB at such a transitional region depends upon some general lowering of the safety factor for propagation (e.g., increased extracellular potassium concentration) such that propagation fails only in the direction where the action potential encounters an increased electrical load.

For UB type II, we assume that the tissue is homogeneous in its geometry, coupling resistance, and excitability properties, and then some lesion with an asymmetrical spatial distribution is imposed on the tissue. The experiments of Downar and Waxman (1976) provide the most controlled study of this type of UB. They applied either external cooling or pressure in an asymmetrical fashion such that there was a gradual progression of injury from left to right as shown in the lower part of Fig. 1, but an abrupt transition from right to left. They showed that UB resulted consistently and reversibly in the direction of the gradual increase in the severity of the lesion. The explanation given by Downar and Waxman for this phenomenon was that an asymmetrical distribution of excitation threshold had developed and that failure of propagation preferentially occurred when the region of highest threshold was approached gradually (left to right in the figure) because the action potential was weakened by the gradual transition in threshold, whereas an action potential traveling from right to left was able to traverse the region of maximal injury more easily because it was able to produce more excitatory current for propagation. This explanation was supported by the modeling of van Capelle and Janse (1976) in which, in an analogue cable model of a cardiac strand, UB developed when a progressive series of leakage conductances was inserted in parallel with the analogue circuits corresponding to the membrane segments.

In the present work, we focus on the second type of UB and address the question: "What parameters of cardiac tissue, when changed in an asymmetrical fashion along the length of an unidimensional strand, produce unidirectional block?" The model we use consists of a

computer simulation of a strand of cardiac tissue with standard membrane parameters represented by the model of Beeler and Reuter (1977) and cable parameters typical of cardiac tissue (Schanne and Ruiz P.-Ceretti, 1978). Asymmetrical lesions can be produced in a controlled fashion by specifying values of some parameters as an arbitrary function of distance along the strand, allowing us to systematically evaluate the relative contribution of each parameter to the possible mechanisms of UB.

METHODS

The strand of cardiac tissue is represented by a set of simultaneous algebraic difference equations, one for each of the 100–200 segments into which the strand is divided. Each segment represents the total area of membrane over a segment length, ΔX (25–100 um), with an effective cell radius, a, of 2.5 um. Each segment has a set of equations (Beeler and Reuter, 1977) that specify the membrane conductances (and thus the membrane current) as functions of voltage and time. At each time step (ΔT = 10 μs) the membrane current is computed for each segment and then the new voltage for each segment is computed, using these currents and the set of simultaneous partial differential equations by a modification of the Crank-Nicholson (1947) implicit integration method. (See Joyner et al., 1978; Sharp and Joyner, 1980; for details of the integration method.) The spatial increment was chosen as either 25 um (length of a single cell) or a higher number (up to 100 um) if the parameters modified did not affect the resting length constant (normally ~550 um). As long as the ratio of the segment length to the resting length constant remained <0.1, neither the action potential shape nor the conduction velocity was changed by the value of the segment length chosen. Similarly, variations in T below 10 μs did not change these parameters.

The simulation method is very flexible, allowing parameters such as R_i (the longitudinal resistance) and $\bar{g}_{Na}$ (the maximum sodium conductance) to be specified as functions of distance along the strand. Other parameters, such as additional leakage conductance, can be added to selected segments of the strand. We stress, however, that there is not sufficient data available for any region of the heart of any species to make a quantitative model for propagation through that region. Measurements of membrane properties related to excitation show a large variability as do the measurements of cable properties. Our choice for a standard model of excitability was formulated from a synthesis of voltage clamp data, resistance measurements, and some assumptions concerning the kinetics of the fast sodium conductance (Beeler and Reuter, 1977). The parameters we chose for C_m (1 μF/cm^2) and R_i (200 Ω cm) are representative. In particular, our choice for the standard R_i does not affect the results presented here on symmetry of conduction except as might be expected by its effect on the resting length constant.

RESULTS

Propagation for a Homogeneous Strand

Fig. 2 *A* shows the results for a homogeneous strand of tissue composed of 100 segments. Stimulation was applied to the left end (segment one) and the membrane potential vs. time is plotted for every 10th segment with the curves displaced vertically for clarity and labeled with the corresponding segment number. The action potential propagates with uniform shape and conduction velocity (38 cm/s). The waveform of the propagating action potential (PAP) is nearly identical to that of the membrane action potential (MAP) resulting from the solution of the Beeler-Reuter model for an isolated isopotential membrane patch, the difference being that the PAP has a decreased spike amplitude due to the normal loading effect of the cable properties.

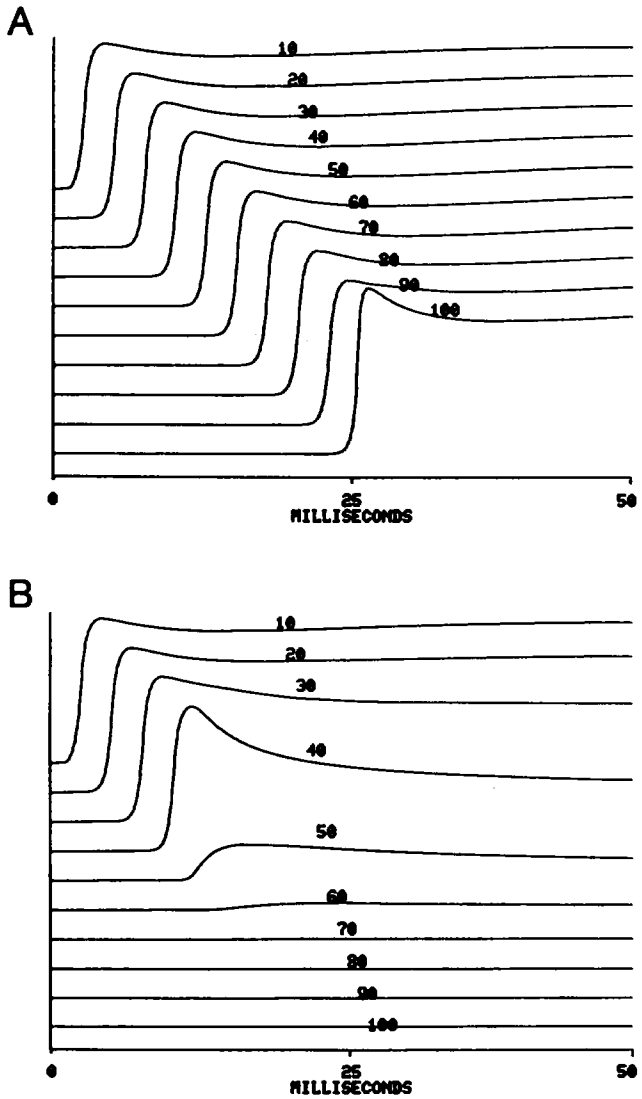

FIGURE 2 Plots of membrane potential vs. time for a series of points at 1-mm intervals along a strand of cardiac tissue (Beeler-Reuter ventricular model). Diameter = 5μm, ΔT = 10 μs, segment length = 100 μm. Curves are shifted vertically with corresponding segment numbers labeled. For *A*, the strand is uniform, whereas for part *B*, $\bar{g}_{Na}$ = 0 for segments 45–55 (a 1-mm length).

Symmetrical Changes in $\bar{g}_{Na}$

Fig. 2 *B* is an illustration of propagation failure produced by a regional decrease in $\bar{g}_{Na}$. For this strand, $\bar{g}_{Na}$ was set equal to zero for the central 1.0 mm of the strand. As the PAP approaches the lesion there is a decreased rate of rise, a decreased spike amplitude, and a marked shortening of the action potential duration. With a shorter lesion, propagation might be successful, although the PAP would still show the decreased rate of rise and decreased

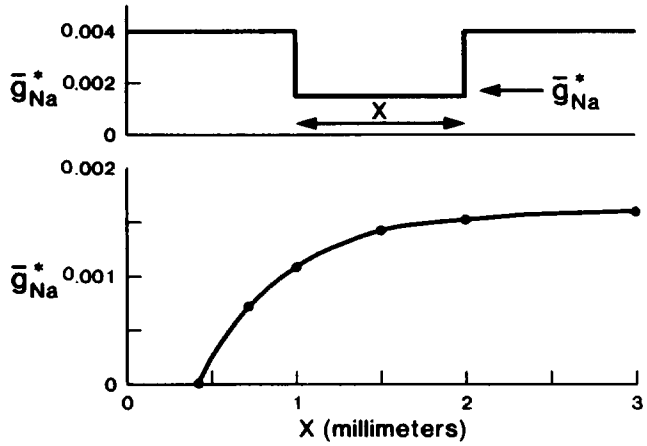

FIGURE 3 Relationship between the minimal value of $\bar{g}^*_{Na}$ and the length X (for the central region of the strand) for which propagation will succeed. Diameter = 5 μm, ΔT = 10 μs, segment length = 100 μm.

spike amplitude as it approached the "depressed" region. The effect of the length of the lesion on the critical value of $\bar{g}_{Na}$ over the lesion is shown in Fig. 3.

Asymmetrical Changes in $\bar{g}_{Na}$

The maximum sodium conductance was varied along the strand as shown in Fig. 4. Fig. 4 *A* is a diagram showing $\bar{g}_{Na}$ as a function of distance, with a normal region followed by a region (of

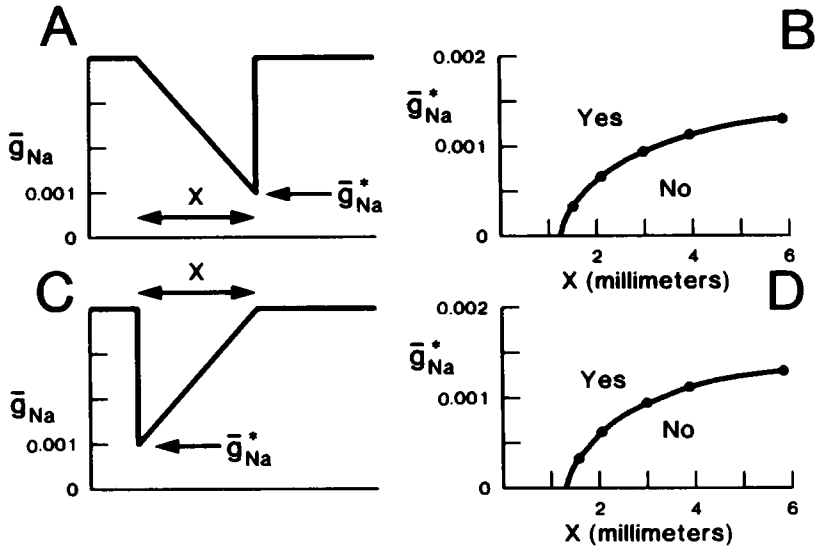

FIGURE 4 Effects of asymmetrical changes in $\bar{g}^*_{Na}$. The relationship between the critical value of $\bar{g}^*_{Na}$ for propagation success and the length X over which the transition occurs is shown in the upper right for the orientation of the lesion as shown in the upper left. The relationship plotted in the lower right is for the orientation of the lesion as diagrammed in the lower left. Stimulation occurred at the left end of the strand in all cases. The Beeler-Reuter model was used with diameter = 5 μm, ΔT = 10 μs, segment length = 25 μm.

length X) over which $\bar{g}_{Na}$ was decreased gradually to a minimal value of $\bar{g}^*_{Na}$, then abruptly returned to the normal value for the rest of the strand. For this simulation (and for all simulations using a regional change in some parameter) the region with varied properties is preceded and followed by long regions (greater than five length constants) of normal properties. We ran a series of simulations like those of Fig. 3 in which, for each value of X, we found the largest value of $\bar{g}^*_{Na}$ for which propagation failed; this relationship is shown in Fig. 4 *B*. Similarly, when we reversed the orientation of the lesion (Fig. 4 *C*) we got the relationship between X and the critical value of $\bar{g}^*_{Na}$ (Fig. 4 *D*). Note that in all of the simulations reported here we are stimulating the left end of the strand, with resulting left to right propagation. We were able to simulate UB with this type of asymmetrical lesion of $\bar{g}^*_{Na}$, but for a given value of X, the range of $\bar{g}^*_{Na}$ over which UB occurred was very small, as shown by the similarity of the relationships for the two orientations of the lesion. In Table I we show the critical ratio $\bar{g}^*_{Na}$/(normal $\bar{g}_{Na}$) for failure of propagation with the lesion orientation of Fig. 4 *A* (gradual entry) or that of Fig. 4 *C* (abrupt entry) for various values of X. In all cases, there was a narrow range of $\bar{g}^*_{Na}$ values over which propagation for the gradual entry would fail while propagation for the abrupt entry was maintained.

Asymmetrical Change in Leakage Conductance, g_L

We added a leakage conductance, g_L, to the Beeler-Reuter model for the membrane properties of each segment, with g_L a function of distance along the strand. We used the normal resting potential as the equilibrium potential for g_L to avoid the effects of steady depolarization had some more positive potential been chosen. Fig. 5 shows g_L as a function of distance along the strand (Fig. 5 *A*) with a region where $g_L = 0$, then a region (of length X) over which g_L gradually increases to a maximum value g^*_L, then a second region with $g_L = 0$. For Fig. 5 *B*, we found, for each value of X, the minimum value of g^*_L at which propagation failed. Fig. 5 *D* shows the results for the reversed orientation of the lesion (Fig. 5 *C*). Similar to the results for asymmetrical changes in $\bar{g}^*_{Na}$, we found only a very narrow range of g_L values, for each X value, over which UB could be produced.

Asymmetrical Changes in Electrical Load

In contrast, asymmetrical changes in the effective cell radius or of the intercellular resistance produced UB over a wide range of parameter values, as illustrated in Figs. 6 and 7. For Fig. 6, we varied the cell radius, a, along the strand. Fig. 6 *A* shows one orientation of the change, with the corresponding relationship between X and the critical maximum radius a^* shown in

TABLE I
FRACTIONAL DECREASE OF $\bar{g}_{Na}$ (OVER A LENGTH X) REQUIRED TO BLOCK PROPAGATION—THE SPATIAL PROFILE OF $\bar{g}_{Na}$ IS ASYMMETRICAL*.

X	$\bar{g}^*_{Na}$/(normal $\bar{g}_{Na}$)	
	Gradual entry	Abrupt entry
2	0.12	0.10
4	0.26	0.24

*See Fig. 4.

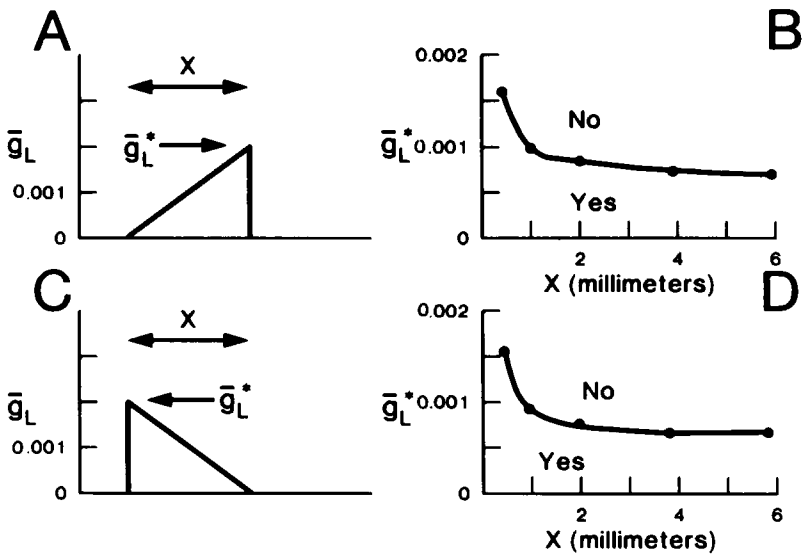

FIGURE 5 Effects of asymmetrical changes in g_L. A leakage conductance was added to the Beeler-Reuter model (equilibrium potential = resting potential) and scaled asymmetrically along the fiber length as shown in the diagrams in the upper and lower left. The corresponding relationships between the critical value of g_L^* for successful propagation and the length, X, over which the transition occurs are shown in the upper and lower right.

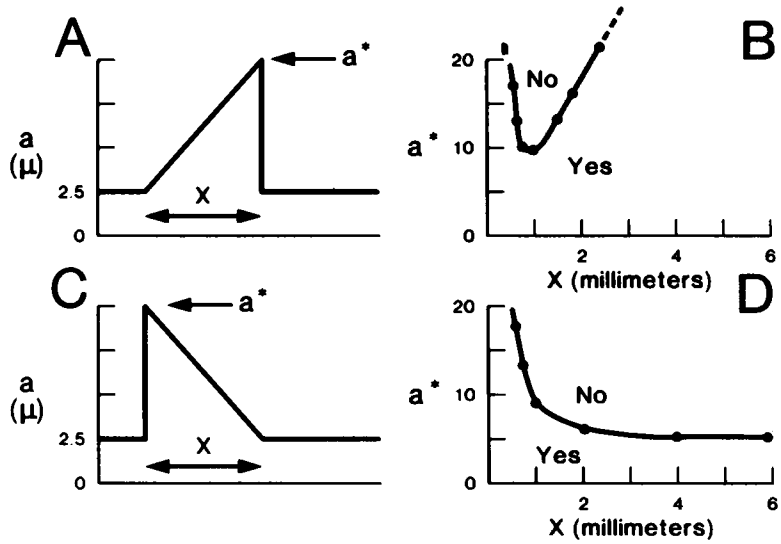

FIGURE 6 Effects of asymmetrical changes in cell radius. The cell radius was changed along the strand as shown in the diagrams in the upper and lower left. The Beeler-Reuter model with standard longitudinal resistivity (R_i = 200 Ω cm) was used for the entire strand. The corresponding relationships between the critical value of a^* in μm for propagation success and the length over which the transition occurs are shown in the upper and lower right.

Fig. 6 *B*. Fig. 6 *C* shows a reversed orientation of the asymmetrical change in radius with the corresponding relationship between X and the critical a^* (Fig. 6 *D*). For small values of X (less than about one resting length constant) the region of increased radius acts as a localized electrical load and block is produced symmetrically. However, for larger values of X, the critical value of a^* increases markedly when the asymmetrical change has the orientation of Fig. 6 *A*, whereas for the orientation of Fig. 6 *C*, the critical value of a^* decreases, leading to a wide range of a^* values over which UB occurs.

Because the electrical load, G_{in}, of the cable is inversely related to the square root of the intercellular resistance and directly related to the 3/2 power of the radius, we would expect that the effects of a twofold increase in radius would be similar to those produced by an eightfold decrease in R_i. As discussed later, we are interested in regional increases in R_i rather than regional decreases. The same principles apply in either case, however, since for a regional increase in R_i the action potential will encounter a decreased electrical load upon entering the region but must then encounter an increased electrical load upon exiting from the region. Therefore, one might expect that, since there was preferential propagation success for the asymmetrical increase in radius if the PAP encountered the increased radius gradually, there will be preferential propagation failure for an asymmetrical increase in R_i if the PAP encounters the increased R_i gradually. The results are shown in Fig. 7 in the same format as Figs. 4–6 and confirm that expectation.

DISCUSSION

Rationale for Use of a One-Dimensional Model

We approach this project with a great respect for the complex multidimensional nature of the heart. However, in the same sense that experimental work has progressed by a reduction to simple geometries (e.g., propagational studies on strands, voltage clamp of isopotential regions), there must be a logical progression of modeling from the isopotential membrane action potential to the simulation of wavefronts moving through a complex syncytium. The preparations in which UB has been observed experimentally have been studied as one-dimensional systems (Cranefield, 1973; Downar and Waxman, 1976; Jalife and Moe, 1976, 1979; Lieberman et al., 1973; Mendez et al., 1969). There are certain regions of the heart (e.g., Purkinje strands, ventricular trabecular) in which experimental studies have shown a one-dimensional electrotonic spread of current (Weidmann, 1952; 1970) and a one-dimensional propagation of action potential (Spach et al., 1973). The cable equation which forms the basis for one-dimensional modeling can be easily extended to two or more dimensions (Joyner et al., 1975; Spach et al., 1979), but for this paper we have presented one-dimensional results for the following reasons: (*a*) avoidance of unnecessary computational complexity; (*b*) more direct applicability to experimental studies; and (*c*) as a necessary intermediate step in understanding more complex geometries.

Rationale for Use of the Beeler-Reuter Model

This model (Beeler and Reuter, 1977) was formulated as a synthesis of voltage clamp data with some additional assumptions to account for the "typical" shape of a ventricular action potential under isopotential conditions. The most arbitrary part of this model is, of course, the kinetics of the fast sodium system, since the temporal resolution and spatial control of cardiac

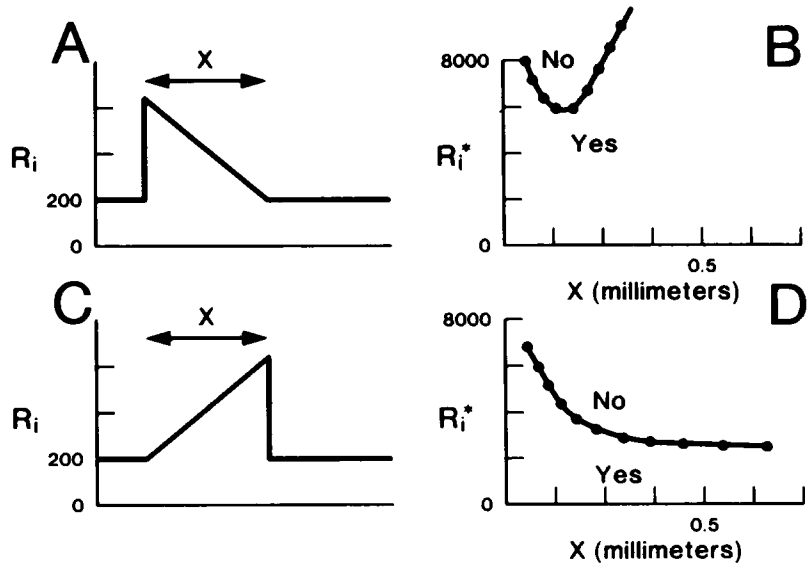

FIGURE 7 Effects of asymmetrical changes in longitudinal resistivity, R_i. In a strand with constant radius, we varied R_i along the length as shown in the diagrams in the upper and lower left. The corresponding relationships between the critical value of R_i^* for propagation success and the length, X, over which the transition occurs are shown in the upper and lower right.

voltage clamping do not allow direct measurements of these parameters. (See Lee et al., 1979, or Colatsky and Tsien, 1979, for more recent progress.) Although the Beeler-Reuter model was formulated for an isopotential region, its applicability as a propagational model is limited only to the extent that the cable properties of the syncytium can be accurately represented by a method such as we have used. However, it should be noted that our results apply quantitatively only to this particular membrane model as a representation of the membrane properties of ventricular cells. It is for this reason that we have concentrated on understanding mechanisms of UB rather than on determining precise conditions under which UB will or will not occur. One result we have presented is that a spatially asymmetrical change in R_i can lead to UB. This result would not depend upon the specific representation of the inward currents (we obtained a similar result using the Hodgkin-Huxley (1952) equations for an axon simulation). Another result was that a regional decrease in $\bar{g}_{Na}$ could produce block, but if $\bar{g}_{Na}$ was decreased in a spatially asymmetrical pattern (as for R_i) the block still appeared to be nearly symmetrical. This result was also tested using the Hodgkin-Huxley model with similar results. (For an axon of 5μm diameter and a temperature of 16°C, a spatially asymmetrical decrease [Fig. 4] in $\bar{g}_{Na}$, over a 5-mm length, produced block for the direction of abrupt entry into the lesion when the minimal $\bar{g}_{Na}$ was 13% of normal, while block occurred for the direction of gradual entry when the minimal $\bar{g}_{Na}$ was 16% of normal.) As with the B-R model, propagation with the H-H model became unidirectional (with minimal $\bar{g}_{Na}$ being between 13 and 16% of normal) with conduction only in the direction of abrupt entry into the lesion. It appears that the phenomenon of nearly symmetrical block being produced by asymmetrical changes in the membrane parameters determining threshold is relatively insensitive to the exact description of the conduction kinetics.

Discussion of Results

It is clear that regional ischemia produces changes in many parameters of cardiac tissue (see review by Carmeliet, 1978) including changes in membrane electrical parameters (e.g. decreased excitability and changes in action potential duration). Concomitant increases in intercellular resistance have been reported by Childers et al. (1979) and might also be inferred from increases in intercellular resistance in response to lowered intracellular pH (Spray et al., 1981), or increased intracellular concentrations of sodium or calcium (Weingart, 1975; de Mello, 1976). The association of often fatal arrhythmias with myocardial infarction has led many investigators to attempt to explain phenomena such as UB and reentry on the basis of regional changes in tissue properties such as are produced by ischemia. What we have done in this paper is to evaluate the relative importance of asymmetrical distribution of a variety of "lesions" to the development of UB.

Although it is certain that the decrease in excitability produced by ischemia is more complex than either a decrease in $\bar{g}_{Na}$ or an increase in a leakage conductance, g_L, (we have specifically excluded the study of regional depolarization), these changes do produce a decrease in excitability whether this decrease is defined by an increased voltage threshold or an increase in required stimulation current. Other parameters could also affect threshold, but these two were chosen as simple mechanisms to decrease the inward current or to increase the outward current at membrane potentials near the normal threshold level. Our results for simulation of asymmetrical changes in these parameters could be interpreted as being in agreement with the modeling of van Capelle and Janse (1976) and with the proposed explanation of the mechanism of UB presented by Downar and Waxman (1976) on the basis of their experimentation with asymmetrical lesions on cardiac strands. However, we found only minimal effects of the orientation of the lesion on propagation, with a slight preference for propagation failure in the direction of gradual increase in severity of the lesion, leading us to believe that this is not a likely mechanism for UB. We suggest an alternative explanation of the data from Downar and Waxman (1976), namely that the critical parameter which is changed asymmetrically by the asymmetrical application of external cooling or pressure is not the threshold per se but the effective longitudinal resistance.

Failure of propagation of an action potential beyond a particular site must be related to the amount of longitudinal charge transferred (time integral of longitudinal current) compared to the amount of charge needed to bring the potential of the adjacent membrane region up to its threshold level for regenerative excitation. With the safety factor for propagation discussed in terms of charge transferred, we can qualitatively analyze the effects of spatial asymmetries in various parameters. The minimal effects of asymmetrical changes in threshold on the production of UB can be explained by reference to Fig. 8 at point A, where we have drawn an asymmetrical change in the threshold as a function of distance along the strand. Considering the critical features to be summarized as the success or failure of propagation from point A to point B (for stimulation at the left end) and from point B to point A (for stimulation at the right end), we can describe two compensating effects which tend to prevent the occurrence of UB. If we define Q_{supp} (LR,A) as the charge that can be supplied by point A to point B during left to right propagation, and Q_{needed} (LR,B) as the charge needed to excite B for left to right propagation; and, Q_{supp} (RL,B) and Q_{needed} (RL,A) in a similar fashion for right to left

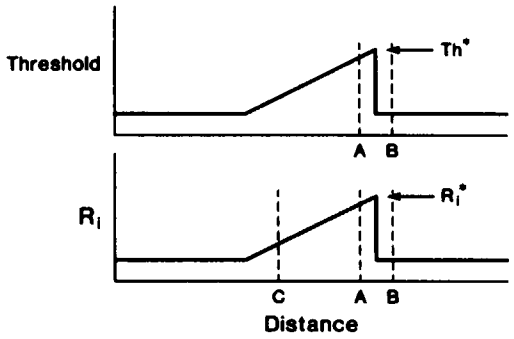

FIGURE 8 Diagrammatic representations of two types of "lesions" considered, both with asymmetrical spatial distributions. Either threshold or longitudinal resistivity are increased to maximal values Th* or R_i^* as shown. See text for discussion of points A, B, and C. Horizontal and vertical scales are in arbitrary units.

propagation, then the necessary condition for identical safety factors for propagation left to right vs. right to left is:

$$\frac{Q_{supp}\,(LR,A)}{Q_{needed}\,(LR,B)} = \frac{Q_{supp}\,(RL,B)}{Q_{needed}\,(RL,A)}.$$

For the purpose of this illustration, we consider each of the regions A and B to be an R-C circuit with some coupling resistance. Assuming the membrane capacitance and area to be fixed, then the Q_{needed} for each area is simply determined by $Q = CV$ with V being the threshold for activation, and thus Q_{needed} (and similarly Q_{supp}) is in units of Coulombs and can be considered as the time integral of an axial current. Thus, considering left to right propagation, there are two factors which could decrease Q_{supp} (LR,A): a decrease in the amount of inward current during activation at point A, or an increase in the coupling resistance between points A and B. Similarly, Q_{needed} (LR,B) would be increased by factors which raised the threshold for point B but would not be affected by the resistive coupling between A and B.

Considering now the effect of increasing the magnitude of the maximum threshold (Th*), we see that this does not affect Q_{needed} (LR,B) or Q_{supp} (RL,B), but will decrease Q_{supp} (LR,A) and increase Q_{needed} (RL,A), and thus the ratios will tend to remain equal, preventing the occurrence of UB. In contrast, the same analysis for the asymmetrical change in R_i diagrammed in part B shows that Q_{needed} (LR,B) remains that same; Q_{needed} (RL,A) and Q_{supp} (LR,A) both decrease because of the decreased length constant (and corresponding decreased spatial extent of the active region) near point A. Q_{supp} (RL,B) also is decreased due to the increased resistance between point B and point A. Thus, as R_i^* is increased, the safety factor for propagation right to left stays about the same while the safety factor for propagation left to right is decreased. Failure of propagation in a right to left direction requires extremely high values of R_i^* (cf., Fig. 7 *A, B*) such that the increased electrical load encountered traveling from point B to point C, although encountered gradually, is sufficient to lower the safety factor below unity.

SUMMARY

The simulations reported here indicate that the mechanisms that could produce UB include spatially asymmetrical changes in the effective longitudinal resistance, R_i. Our results predict the occurrence of UB with simple asymmetrical changes in excitation threshold only within a very narrow range of parameter values, but there are certainly enough uncertainties with the Beeler-Reuter model and the cable representation that we cannot rule out the possibility that the real tissue may have a wider range of parameter values over which UB occurs with this type of lesion. The simulations of UB with graded changes in R_i provide an alternative explanation for the data of Downar and Waxman (1976) for the production of UB with asymmetrical graded changes in temperature or pressure.

This work was supported by National Institutes of Health grant HL22562.

Received for publication 21 December 1979 and in revised form 12 March 1981.

REFERENCES

Beeler, G. W., and H. Reuter. 1977. Reconstruction of the action potential of myocardial fibers. *J. Physiol. (Lond.).* 268:177–210.

Carmeliet, E. 1978. Cardiac transmembrane potentials and metabolism. *Circ. Res.* 42:577–587.

Childers, R. W., T. Cope, R. Lyon, and R. Holland. 1979. Tissue resistance in ventricular ischemia. *Circulation.* 60 (Suppl. II):10. (Abstr.)

Colatsky, T. J., and R. W. Tsien. 1979. Sodium channels in rabbit cardiac Purkinje fibres. *Nature (Lond.).* 278:265–278.

Cranefield, P. F., A. L. Wit, and B. F. Hoffman. 1973. Genesis of cardiac arrhythmias. *Circulation.* 47:190–205.

Crank, J., and P. Nicholson. 1947. A practical method for numerical evaluation of solutions of partial differential equations of the heat-conduction type. *Proc. Cambridge Phil. Soc.* 43:50–67.

De la Fuente, D., B. I. Sasyniuk, and G. K. Moe. 1971. Conduction through a narrow isthmus in isolated canine atrial tissue. A model of the WPW syndrome. *Circulation.* 46:803–809.

de Mello, W. C. 1976. Influence of the sodium pump on intercellular communication in heart fibers: effect of intracellular injection of sodium ion on electrical coupling. *J. Physiol. (Lond.).* 263:171–197.

Downar, E., and M. B. Waxman. 1976. Depressed conduction and unidirectional block in Purkinje fibers. *In* The Conduction System of the Heart. H. J. J. Wellens, K. I. Lie, and M. J. Janse, Editors. Lea & Febiger, Philadelphia. 393–409.

Hodgkin, A. L., and A. F. Huxley. 1952. The components of membrane conductance in the giant axon of *Loligo. J. Physiol. (Lond.).* 116:473–496.

Jalife, J., and G. K. Moe. 1976. Effect of electrotonic potentials on pacemaker activity in canine Purkinke fibers in relation to parasystole. *Circ. Res.* 39:801–808.

Jalife, J., and G. K. Moe. 1979. A biological model of parasystole. *Am. J. Cardiol.* 43:761–772.

Joyner, R. W., F. R. Ramon, and J. W. Moore. 1975. Simulation of action potential propagation in an inhomogeneous sheet of electrically coupled excitable cells. *Circ. Res.* 36:654–661.

Joyner, R. W., R. M. Westerfield, J. W. Moore, and N. Stockbridge. 1978. A numerical method to model excitable cells. *Biophys. J.* 22:155–170.

Lee, K. S., T. A. Weeks, R. L. Kao, N. Akaike, and A. M. Brown. 1979. Sodium current in single heart muscle cells. *Nature (Lond.).* 278:269–271.

Lieberman, M., J. M. Kootsey, E. A. Johnson, and T. Sawanobori. 1973. Slow conduction in cardiac muscle: a biophysical model. *Biophys. J.* 13:37–55.

Mendez, C., W. J. Mueller, J. Meredith, and G. K. Moe. 1969. Interaction of transmembrane potentials in canine Purkinje fibers and at Purkinje fiber-muscle junctions. *Circ. Res.* 24:361–372.

Ramon, R., R. W. Joyner, and J. W. Moore. 1976. Propagation of action potentials in inhomogeneous axon regions. *Fed. Proc.* 34:1357–1363.

Schanne, O. F., and E. Ruiz P.-Ceretti. 1978. Impedance Measurements in Biological Cells. John Wiley & Sons, Inc., New York.

Scherf, D., and J. Cohen. 1964. The Atrioventricular Node and Selected Cardiac Arrhythmias. Grune & Stratton, Inc., New York.

Schmitt, F. O., and J. Erlanger. 1928. Directional differences in the conduction of the impulse through heart muscle and their possible relation to extrasystolic and fibrillatory contractions. *Am. J. Physiol.* 87:326–340.

Sharp, G. H., and R. W. Joyner. 1980. Simulated propagation of cardiac action potentials. *Biophys. J.* 31:403–423.

Spach, M. S., W. T. Miller, III, E. Miller-Jones, R. B. Warren, and R. C. Barr. 1979. Extracellular potentials related to intracellular action potentials during impulse conduction in anisotropic canine cardiac muscle. *Circ. Res.* 45:188–204.

Spray, D. C., A. L. Harris, and M. V. L. Bennett. 1981. Gap junctional resistance is a simple and sensitive function of intracellular pH. *Science (Wash., D.C.).* 211:712–715.

van Capelle, F. J. L., and M. J. Janse. 1976. Influence of geometry on the shape of the propagated action potential. *In* The Conduction System of the Heart. H. J. J. Wellens, K. I. Lie, and M. J. Janse, editors. Lea & Febiger, Philadelphia. pp. 316–335.

Watanabe, Y. 1971. Reassessment of parasystole. *Am. Heart J.* 81:451–462.

Weidman, S. 1970. Electrical constant of trabecular muscle from mammalian heart. *J. Physiol. (Lond.).* 210:1041–1054.

Weidman, S. 1952. The electrical constants of Purkinje fibers. *J. Physiol. (Lond.).* 118:348–360.

Weingart, R. 1975. Electrical uncoupling in mammalian heart muscle induced by cardiac glycosides. *Experentia (Basel).* 31:715.

Westerfield, R. M., R. W. Joyner, and J. W. Moore. 1978. Temperature-sensitive conduction failure at axon branch points. *J. Neurophysiol.* 41:1–8.